

Experimental and Computational Study of the Effect of Alcohols on the Solution and Adsorption Properties of a Nonionic Symmetric Triblock Copolymer

Xiaomeng Liu,[†] Feng He,[§] Carlos Salas,[†] Melissa A. Pasquinelli,^{*,‡} Jan Genzer,[§] and Orlando J. Rojas^{*,†,||}

[†]Department of Forest Biomaterials, North Carolina State University, Raleigh, North Carolina 27695, United States

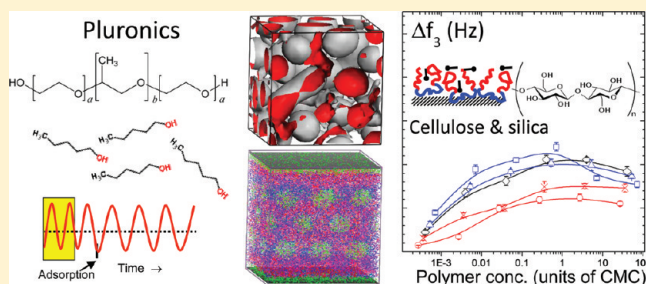
[‡]Department of Textile Engineering, Chemistry and Science, North Carolina State University, Raleigh, North Carolina 27695, United States

[§]Department of Chemical & Biomolecular Engineering, North Carolina State University, Raleigh, North Carolina 27695, United States

^{||}Faculty of Chemistry and Materials Sciences, Department of Forest Products Technology, Aalto University, P.O. Box 16300, 00076 Aalto, Finland

Supporting Information

ABSTRACT: This study investigates the effect of alcohols on the solution and adsorption properties of symmetric triblock nonionic copolymers comprising blocks of ethylene oxide (EO) and propylene oxide (PO) ($\text{EO}_{37}\text{PO}_{56}\text{EO}_{37}$). The cloud point, surface tension, critical micelle concentration (CMC), and maximum packing at the air–water interface are determined, and the latter is compared to the amount of polymer that adsorbs from solution onto polypropylene (PP) and cellulose surfaces. The interaction energy and radius of micelles are calculated by using molecular dynamics (MD) simulations. Equivalent MD bead parameters were used in dynamic density functional theory (DDFT) simulations to study the influence of alcohols on the phase behavior of $\text{EO}_{37}\text{PO}_{56}\text{EO}_{37}$ and its adsorption on PP from aqueous solutions. The simulation results agree qualitatively with the experimental observations. Ethanol acts as a good cosolvent for $\text{EO}_{37}\text{PO}_{56}\text{EO}_{37}$ and reduces the amount of $\text{EO}_{37}\text{PO}_{56}\text{EO}_{37}$ that adsorbs on PP surfaces; however, little or no influence is observed on the adsorption on cellulose. Interestingly, longer chain alcohols, such as 1-pentanol, produce the opposite effect. Overall, the solution and adsorption properties of nonionic symmetric triblock copolymers in the presence of alcohols are rationalized by changes in solvency and the hydrophobic effect.



INTRODUCTION

Triblock copolymers of poly(ethylene oxide)–poly(propylene oxide)–poly(ethylene oxide) (PEO–PPO–PEO or $\text{EO}_n\text{PO}_m\text{EO}_n$) are used widely in the chemical and pharmaceutical industries in the formulations of detergents, colloidal dispersion stabilizers,^{1,2} cosmetics, and drug-delivery products.³ Key to their applications are the amphiphilic properties of $\text{EO}_n\text{PO}_m\text{EO}_n$ macromolecules, which enable the formation of macromolecular assemblies with tailorabile surface affinity to surfaces and to the solution media. Recent interest in this area has focused on the design and creation of functional, adsorption-driven, self-assembled nanostructures.^{4–6} Therefore, understanding the relationship between bulk and interfacial behavior of such macromolecules is critical in the design of new functionalities.

Atomic force microscopy (AFM),^{7,8} surface plasmon resonance,^{7–9} and quartz crystal microbalance⁸ have been employed to study the adsorption of $\text{EO}_n\text{PO}_m\text{EO}_n$ block copolymers at the solid–liquid interface. The structure of adsorbed triblock copolymer layers has been observed to be highly dependent on

the relative length of the hydrophilic and hydrophobic blocks of the copolymer.^{7,9} In our previous work, $\text{EO}_{37}\text{PO}_{56}\text{EO}_{37}$ was found to adsorb on a hydrophobic surface as a monolayer, while micellar structures were partitioned on hydrophilic surfaces.⁸ Overall, $\text{EO}_{37}\text{PO}_{56}\text{EO}_{37}$ adsorbed to a larger extent onto the more hydrophobic surfaces; in such cases, a viscoelastic adsorbed layer with a large amount of coupled water was observed.

Insights into the interactions and adsorption of polymers at interfaces have been obtained experimentally; however, computational modeling can expand further in areas that are elusive to experiments. Atomistic simulations allow for elucidation of structural and thermophysical properties of multiparticle systems, while mesoscale simulations facilitate investigations at larger length and time scales. Mesoscopic dynamics (MesoDyn),^{10–12} a coarse-grained simulation method based on dynamic density

Received: July 27, 2011

Revised: November 25, 2011

Published: December 21, 2011

functional theory, has been used to study microphase separation and micelle formation. Several MesoDyn efforts have been reported on the solution properties of $\text{EO}_n\text{--PO}_m\text{--EO}_n$ block copolymers with different combinations of molar numbers m and n : $\text{EO}_{34}\text{PO}_6\text{EO}_{34}$,¹³ $\text{EO}_{37}\text{PO}_{56}\text{EO}_{37}$,¹³ $\text{EO}_{30}\text{PO}_{13}\text{EO}_{30}$,¹⁴ $\text{EO}_{29}\text{PO}_{18}\text{EO}_{29}$,¹⁵ $\text{EO}_{26}\text{PO}_{40}\text{EO}_{26}$,¹⁵ $\text{EO}_{17}\text{PO}_{60}\text{EO}_{17}$,¹⁵ $\text{EO}_{19}\text{PO}_{69}\text{EO}_{19}$,¹⁶ and $\text{EO}_{19}\text{PO}_{29}\text{EO}_{19}$.¹⁷

Most of the reported work related to polymer adsorption has been limited to purely aqueous systems. However, very often adsorption occurs in the presence of low molecular weight species, such as cosolvents, cosurfactants, and cosolubilizers. The presence of low molecular weight species is especially pertinent to the formulation of aqueous and nonaqueous colloids, drugs, and cosmetics.¹⁸ The effect of polar organic solvents and cosolutes on the micellization of $\text{EO}_n\text{--PO}_m\text{--EO}_n$ has been addressed in previous reports.^{19–22} Short chain alcohols, such as ethanol, have been found to prevent the formation of $\text{EO}_n\text{--PO}_m\text{--EO}_n$ micelles in aqueous solution,²³ while longer chain alcohols and model adjuvants, such as pentanol, benzyl benzoate, and benzyl alcohol, promoted micellization.^{18,24,25} The effect of other polar organic solvents on the micellization of $\text{EO}_n\text{--PO}_m\text{--EO}_n$ block copolymers has been addressed as well.^{26,27} A relevant MesoDyn mesoscale simulation is that reported for $\text{EO}_{30}\text{PO}_{13}\text{EO}_{30}$ in aqueous solution containing *p*-xylene.¹⁴ While polymolecular micelles were absent in pure *p*-xylene, addition of water to different volume fractions facilitated the formation of associative structures of different shape. In addition, their critical micellization concentration (CMC) was found to be controlled by the type and amount of cosolvent.

To our knowledge, no experimental or computational report is available on the effect of alcohols on the adsorption behavior of $\text{EO}_n\text{--PO}_m\text{--EO}_n$ macromolecules on polymeric surfaces. Therefore, in this work, the effect of alcohols of different chain lengths was investigated in relation to the solution, associative, and adsorption properties of a $\text{EO}_n\text{--PO}_m\text{--EO}_n$ symmetric triblock copolymer on two substrates with different degrees of hydrophilicity and electrostatic charge, i.e., polypropylene and cellulose. In addition, computer simulations at the molecular ($10^{-9}\text{--}10^{-8}$ m) and mesoscopic ($10^{-7}\text{--}10^{-5}$ m) scales were performed to rationalize the experimental results.

MATERIALS AND METHODS

Deionized (DI) water from an ion-exchange system (Pureflow, Inc.) followed by treatment in a Milli-Q Gradient unit with a resultant resistivity of $>18 \text{ M}\Omega\cdot\text{cm}$ was used to prepare the polymer solutions and during QCM experiments (background fluid, rinsing solution, etc.). A symmetrical triblock nonionic copolymer consisting of ethylene oxide (EO) and propylene oxide (PO) blocks, under the trade name of Pluronic P105 ($\text{EO}_{37}\text{PO}_{56}\text{EO}_{37}$), was donated by BASF Corp. and used without further purification. $\text{EO}_{37}\text{PO}_{56}\text{EO}_{37}$ weight-average molecular weight was determined to be 6300 Da with a polydispersity index of 1.04 as determined from size-exclusion chromatography coupled with light scattering.⁸ Ethanol (99.9%) was purchased from Fisher Scientific. The 1-butanol (99.7%), 1-hexanol (99%), and 1-pentanol (98%) were purchased from Sigma-Aldrich.

Aqueous polymer solutions with concentrations ranging from 1×10^{-4} to 10 w/v % were freshly prepared before each experiment. Alcohol was added under stirring to aqueous $\text{EO}_{37}\text{PO}_{56}\text{EO}_{37}$ solutions to attain given concentrations.

QCM gold-coated quartz sensors (Q-Sense Inc., Sweden) were cleaned first with Piranha solution (70% H_2SO_4 + 30% H_2O_2 (30%)) for 20 min followed by UV/ozone treatment (28 mW/cm² at 254 nm wavelength) for 10 min to remove any organic contaminants. Thin films of PP and cellulose were deposited on the clean QCM gold sensors by spin-coating; details about their manufacture can be found in ref 28.

Cloud-Point. Cloud-points (CP) were determined by observing the temperature at which the copolymer solution became turbid upon heating; heating rates of 1–2 °C per minute near the CP were maintained. The average CP after multiple determinations is reported.

Surface Tension. The surface tension of aqueous $\text{EO}_{37}\text{PO}_{56}\text{EO}_{37}$ and alcohol solutions was determined by means of a Cahn balance (Thermo Material Characterization, USA, Madison, WI) equipped with a Pt–Ir Willhelmy plate at 25 °C. The minimum surface tension and the critical micelle concentration (CMC) were determined.

Quartz Crystal Microgravimetry. A quartz crystal microbalance (Q-Sense model E4, Gothenburg, Sweden) was used to measure the rate of adsorption, the adsorbed mass, and the energy dissipation of the adsorbed layers. The principles of the QCM technique have been addressed in detail elsewhere.^{29,30} The changes in resonant frequency f and energy dissipation D of the polymer-coated QCM sensors were measured. The shift in the resonance frequency was used to calculate the areal adsorption by means of the Sauerbrey equation (eq 1),³¹ which is generally applicable if (1) the adsorbed macromolecules form a thin, rigid, and homogeneous layer and (2) the extra mass deposited on the sensor is small compared to that of the resonator (polymer-coated sensor).

$$\Delta m = -\frac{c\Delta f}{n} \quad (1)$$

In eq 1, c represents a constant characteristic of the sensitivity of the resonator to changes in mass (17.7 ng Hz⁻¹ cm⁻² for the used 5 MHz quartz crystals), and n is the overtone number ($n = 1, 3, 5, 7$, etc.).

The change in QCM energy dissipation, D , was used to determine the viscoelastic properties of the adsorbed layer. D was measured after switching off the resonator and by recording the exponential decay in oscillation (frequency and amplitude dampening), which was then used to obtain the energy dissipated and stored during one period of oscillation, $E_{\text{dissipated}}$ and E_{stored} , respectively, according to eq 2

$$D = \frac{E_{\text{dissipated}}}{2\pi E_{\text{stored}}} \quad (2)$$

Energy dissipation can be attributed to (1) changes in the viscoelastic properties of the crystal and adsorbed layer and (2) variations in the density and viscosity of the surrounding solution.²⁹ Changes in f and D were recorded after a rinsing step to replace the adsorbing $\text{EO}_{37}\text{PO}_{56}\text{EO}_{37}$ solution with pure water, thereby allowing the determination of the effective shift in f and D .

The QCM modules and tubing were cleaned for one hour before each run by using a 2% (v/v) Hellmanex solution (Hellma GMBH, Müllheim, Germany). They were then rinsed with ethanol and water. After mounting the respective polymer-coated sensor in the QCM module, water was injected continuously with the system adjusted to a temperature of 25.00 ± 0.02 °C.

In a typical experiment, uniform films of polypropylene and cellulose were first deposited on the QCM gold sensors by spin-coating. The thicknesses and roughness of the respective thin films, under the same operating conditions, were reported in our previous publication.²⁸ The shifts in QCM frequency, both in air and in water, were used to test the quality of the coating before each experiment. Prior to any measurement, the polymer-coated sensors were allowed to equilibrate in water for half a day in order to establish the base *f* and *D* signals, which were then zeroed.

In order to study the adsorption isotherm of EO₃₇PO₅₆EO₃₇ in the presence of alcohol, aqueous solutions of the polymer (concentrations ranging from 1×10^{-4} to 10 w/v %) with alcohol (4 g/L or 8 g/L) were injected into the QCM flow module at a constant flow rate of 0.1 mL/min. The shifts in *f* and *D* were monitored as a function of time for about 15 min, followed by rinsing with pure water. QCM adsorption data were obtained by running single, individual experiments at a given polymer concentration. All adsorption experiments were conducted at least in triplicate, and average values are reported.

Molecular Dynamics Simulations. In order to gain further insights into the phase behavior of EO₃₇PO₅₆EO₃₇ in the presence of ethanol and 1-pentanol, atomistic MD simulations were performed with the software program LAMMPS³² at the High Performance Computing (HPC) Center at North Carolina State University. Ten EO₃₇PO₅₆EO₃₇ chains in the amorphous state were mixed with the solvent (water, water with 32 g/L of ethanol, and water with 32 g/L of 1-pentanol) in a $7 \times 7 \times 7$ nm³ periodic cube using the Amorphous Cell module in Materials Studio software³³ version 5.5. The PCFF³⁴ force field was used for the potential energy terms. The MD simulations were carried out at 298 K for 10 ns with the NVT ensemble, which kept the number of atoms, temperature, and volume constant. After equilibrium, the radius of gyration and the interaction energy were calculated. The interaction energy was defined as the pairwise energy between different group of molecules, which includes the nonbonded energy terms, Columbic, and van der Waals.

To better understand EO₃₇PO₅₆EO₃₇ adsorption on PP, an amorphous PP layer was built with the Amorphous Cell module of Materials Studio by packing 30 repeat units of PP into a $7 \times 7 \times 3$ nm layer with a density of 0.85 g/cm³. The layer was confined at the top and bottom by xenon crystals, which are ultraflat and uniform crystals with inert properties. A geometry optimization and annealing in the range from 300 to 500 K was done to relax the PP layer. Single EO₃₇PO₅₆EO₃₇ chains were placed along the PP surface at a distance of 2 nm and immersed in different solvent conditions: pure water, water and 32 g/L of ethanol mixture, and water and 32 g/L of pentanol mixture, respectively. The MD simulations were carried out at 298 K for 10 ns with the NVT ensemble to allow the system to reach equilibrium.

Mesodyn Simulation Methods. In a MesoDyn simulation, atoms are grouped together as Gaussian springs and beads, where each bead denotes a statistical unit that represents a number of real monomers.¹⁸ This approach involves relatively high computational efficiency and can be extended to scales (both length and time) spanning several orders of magnitude as compared to atomistic MD. The basic theory behind MesoDyn and its application to aqueous EO_nPO_mEO_n polymer solutions has been described in detail by others;^{13,16,35–37} thus, only a brief account is provided here. The MesoDyn simulations were performed with Accelrys' Materials Studio software³³ version 5.5 on a Dell OptiPlex 980 with Intel(R) i7-860 2.80 GHz processors.

Table 1. Bead Interaction Parameters Used in MesoDyn Simulations^a

	water	PEO	PPO	ethanol	pentanol (A)	pentanol (B)
water (W)						
PEO (E)	0.35					
PPO (P)	1.7	3.0				
ethanol (H)	0.01	0.2	1.2			
pentanol (A)	0.01	0.2	1.2			
pentanol (B)	4	2	1.8		2	
PP (S)	6	5	3.8	5	5	2

^aThe diagonal of this table corresponds to the self-interaction parameters, which are not included in MesoDyn.

In this work, the chemical nature of the system was defined via material parameters such as the bead type, self-diffusion coefficients, and the interaction energies of the beads as well as the molecular chain architecture. van Vlimmeren et al.³⁵ established a simple mapping relationship between the atomic and Gaussian chains for EO_nPO_mEO_n copolymers. The numerical monomer/bead ratios were taken as 4.3 and 3.3 for the two PEO and the single PPO blocks, respectively.^{15,16} Therefore, the EO₃₇-PO₅₆EO₃₇ chain was defined as the equivalent E₉P₁₇E₉ Gaussian chain, where bead E and P represent the PEO and the PPO blocks, respectively. For the solvents, both ethanol and water were modeled as a single bead. 1-Pentanol was modeled as two connected beads of pentanol A and pentanol B, where pentanol A includes a hydroxyl and two CH₂ groups, and pentanol B includes the remaining three CH₂ groups.

The pairwise interaction between different bead types in MesoDyn is an important input parameter, which can be related to the Flory-Huggins parameter (χ); the values used in this work are summarized in Table 1. For instance, van Vlimmeren³⁵ estimated the PEO-PPO interaction parameter (χ_{EP}) to be between 3 and 5 from the group contribution method. Thus, we set $\chi_{EP} = 3.0$ for the PPO-PEO interactions. By fitting the experimental PEO-water and PPO-water phase diagrams, values of $\chi_{EW} = 0.65$ and $\chi_{PW} = 1.7$ were extracted at room temperature.^{38–40} However, the polymer is considered to not be easily dissolved in the solvent when $\chi > 0.5$, so Guo and co-workers¹² used $\chi_{EW} = 0.35$ in their work. While large discrepancies in χ_{EW} are noted, the value of χ_{PW} agrees with the one calculated from vapor-pressure data of aqueous homopolymer solutions with the Flory-Huggins expression.⁴¹

$$\chi_{IJ} = \theta^{-2} \{ \ln p/p^0 - \ln(1-\theta) - (1-1/N)\theta \} \quad (3)$$

where p is the vapor pressure, p^0 is the vapor pressure of pure solvent, θ is the polymer volume fraction, and N is the number of monomers per bead. Therefore, the Flory-Huggins parameters were chosen to be $\chi_{EW} = 0.35$ and $\chi_{PW} = 1.7$.

Because of the lack of data on the vapor-pressure of PEO and PPO homopolymers in alcohol solutions, the Flory-Huggins parameters between polymer blocks and the alcohol molecules were calculated with the Blends module of Materials Studio version 5.5. This module utilizes molecular simulations to calculate the energy mixing (ΔE_{mix}) between two substances from the following equation:⁴²

$$\Delta E_{\text{mix}} = \phi_A \left(\frac{E_{\text{coh}}}{V} \right)_A + \phi_B \left(\frac{E_{\text{coh}}}{V} \right)_B - \left(\frac{E_{\text{coh}}}{V} \right)_{\text{mix}} \quad (4)$$

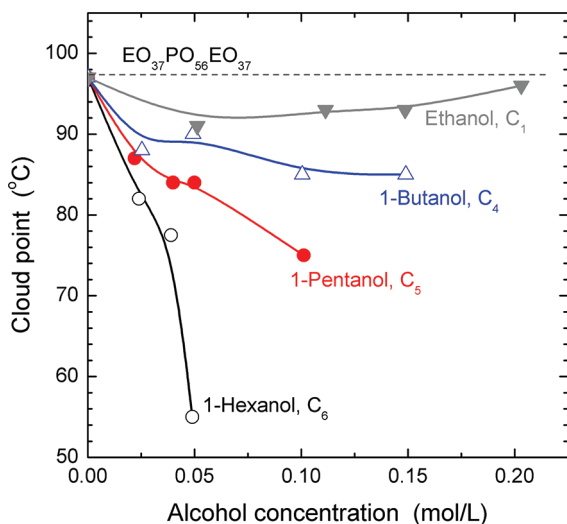


Figure 1. Cloud point of 1% $\text{EO}_{37}\text{PO}_{56}\text{EO}_{37}$ aqueous solution in the presence of different alcohols that were added at a series of concentrations. The solid lines are meant to guide the eye. The dash-dotted line represents the cloud point of 1% $\text{EO}_{37}\text{PO}_{56}\text{EO}_{37}$ in water.

where φ_A and φ_B are the volume fractions of A and B in the mixed system, respectively, and E_{coh} is the cohesive energy. From the energy of mixing, the Flory–Huggins parameter can be calculated from the following equation:

$$\chi = \frac{\Delta E_{\text{mix}}}{RT} \quad (5)$$

The Dreiding force field⁴³ was used for the potential energy terms, as it was found previously to estimate accurately the cohesive energy and solubility parameters.^{40,44} The bead interaction parameters derived from these calculations are given in Table 1.

Adsorption of $\text{EO}_{37}\text{PO}_{56}\text{EO}_{37}$ on a PP surface was also investigated through MesoDyn simulations. A single layer of the lattice at $z = 0$, which represents the PP surface, was introduced. Beads were excluded from the layer, and the interaction parameters between PP and the various beads were defined by the atomistic simulation, which are also given in Table 1.

Other MesoDyn simulation details are as follows. The dimension of the lattice used was $32 \times 32 \times 32 \text{ nm}^3$. The simulation temperature and time steps were set at 298 K and 50 ns, respectively. The noise scaling parameter was set to 100, and the compressibility parameter was set to 10.^{45,46} The bead volume was set to 300 \AA^3 for all beads. The ratio of the bond length, a , and the cell length, h , was automatically set to $a/h = 1.1543$ to ensure isotropy of all grid-restricted operators.³⁶ The bead diffusion coefficients were set to $1.0 \times 10^{-7} \text{ cm}^2/\text{s}$, as used in previous work.^{12,13} A total of 20 000 simulation steps were run, which corresponds to a total time of 1 ms.

RESULTS AND DISCUSSION

Cloud Point of $\text{EO}_{37}\text{PO}_{56}\text{EO}_{37}$ in the Presence of Alcohols. The cloud point (CP) data of aqueous solutions of $\text{EO}_{37}\text{PO}_{56}\text{EO}_{37}$ with and without alcohol are shown in Figure 1. The CP for 1% aqueous $\text{EO}_{37}\text{PO}_{56}\text{EO}_{37}$ solution is found to be close to 98 °C. This value depends on the solubility of the PEO blocks, which typically decreases as the temperature is raised. As far as the effect of alcohol, the changes observed in the CP are found to depend on the number of carbon atoms in the alkyl chain of the

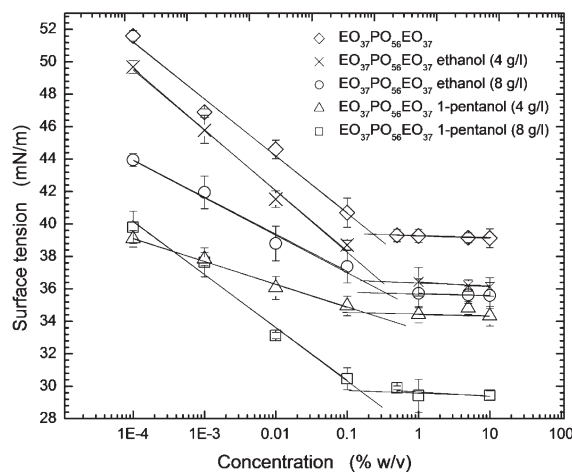


Figure 2. Surface tension isotherms for aqueous solutions of $\text{EO}_{37}\text{PO}_{56}\text{EO}_{37}$ in water (\diamond), ethanol (4 g/L) (\times), and 8 g/L (\circ)), and 1-pentanol (4 g/L) (\triangle) and 8 g/L (\square) solutions measured at 25 °C. The lines are added as guides to the eye.

Table 2. Critical Micelle Concentration (CMC), Free Energy of Micellization (ΔG_m°), and Maximum Packing Density (Surface Excess) at the Air–Water Interface (25 °C) for $\text{EO}_{37}\text{PO}_{56}\text{EO}_{37}$ in Aqueous Solutions with Added Alcohols

	water	ethanol		1-pentanol	
		4 g/L	8 g/L	4 g/L	8 g/L
CMC (% w/v)	0.24	0.28	0.37	0.19	0.14
ΔG_m° (kJ/mol)	-29.54	-29.16	-28.50	-30.14	-31.05
surface excess (molecules/nm ²)	0.39	0.37	0.25	0.18	0.34

alcohol. The addition of a small amount of ethanol to 1% aqueous $\text{EO}_{37}\text{PO}_{56}\text{EO}_{37}$ solution reduces the CP. However, in contrast to other alcohols, the CP increases as the concentration of ethanol is increased further. This trend is likely due to the better solvation of the EO blocks with ethanol. Higher homologues of the alcohol series reduce the CP with increasing alcohol concentration. Similar trends in the CP upon addition of alcohol have been reported for $\text{EO}_{19}\text{PO}_{69}\text{EO}_{19}$.⁴⁷

Surface Tension of $\text{EO}_{37}\text{PO}_{56}\text{EO}_{37}$ in the Presence of Alcohol. Figure 2 provides the surface tension isotherms of an aqueous solution of $\text{EO}_{37}\text{PO}_{56}\text{EO}_{37}$ in the presence of 4 and 8 g/L of ethanol and 1-pentanol. The surface tension isotherm for pure $\text{EO}_{37}\text{PO}_{56}\text{EO}_{37}$ in water is also shown as a reference. The data reveal that the surface activity increased (i.e., the surface tension was lowered) upon the addition of ethanol and 1-pentanol. The critical micelle concentrations (CMC) were obtained from the data in Figure 2 and are listed in Table 2. The CMC of the respective surface-active polymer increased upon the addition of ethanol. Contrary to the effect of ethanol, the addition of 1-pentanol favored micellization of the block copolymer in aqueous solutions, as has been also reported elsewhere.⁴⁸

The surface excess, Γ , at the air–liquid interface was obtained by the Gibbs adsorption equation

$$\Gamma = -\frac{1}{RT} \left(\frac{\partial \gamma}{\partial \ln c} \right)_T \quad (6)$$

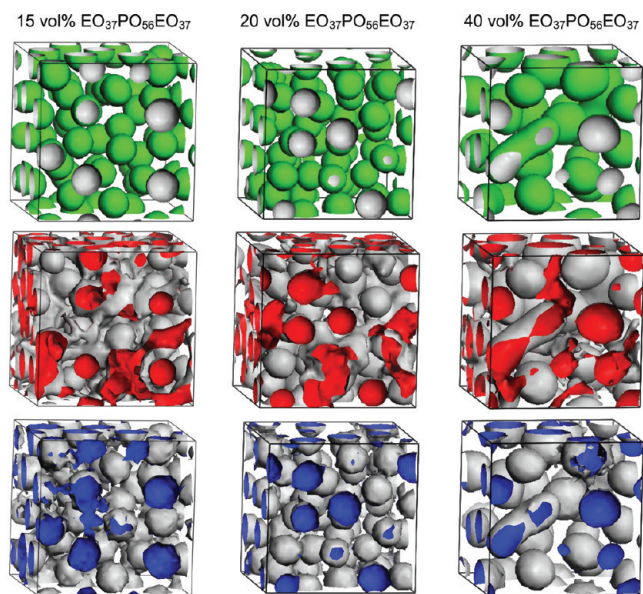


Figure 3. Isosurface of the density field after 20 000 steps of a MesoDyn simulation of a series (15, 20, and 40% by volume) of $\text{EO}_{37}\text{PO}_{56}\text{EO}_{37}$ in pure water at 298 K. The colors indicate the PPO block (green), PEO block (red), and water (blue). All three components are given separately in each row.

where γ is the surface tension in the present case measured at constant temperature of 297 K, R is the universal gas constant, and c is the $\text{EO}_{37}\text{PO}_{56}\text{EO}_{37}$ molar concentration. The calculated surface excess at maximum polymer packing is included in Table 2, which is noted here as a reference for further comparison with the areal adsorption determined at solid–liquid interfaces (see later sections).

A closed association model, which assumes equilibrium between the unimers (molecularly dissolved amphiphiles) and the micelles, has been found to describe satisfactorily the micellization process of PEO–PPO–PEO block copolymers.⁴⁹ The standard free energy change associated with transferring 1 mol of amphiphile from solution to the micelle phase (free energy of micellization), ΔG_m° , in the absence of electrostatic interactions (the case of nonionic amphiphiles) is given by

$$\Delta G_m^\circ = RT \ln(X_{\text{CMC}}) \quad (7)$$

where R is the universal gas constant, T is the absolute temperature, and X_{CMC} is the critical micelle concentration expressed in mole fraction units.

Table 2 includes the standard free energy for $\text{EO}_{37}\text{PO}_{56}\text{PO}_{37}$ in the various solutions as well as the maximum packing at the air–water interface. The addition of ethanol increases the free energy of micellization relative to pure aqueous solution. Ethanol prevents the formation of micelles, while the addition of 1-pentanol produces the opposite effect. The higher CMC observed after the addition of ethanol indicates that better solvency for the PEO–PPO–PEO block copolymer exists in this case. Ethanol with water, being a good solvent for PEO,^{24,50} swells the PEO blocks and prevents self-association of the block copolymer into micelles. In contrast, the decrease of CMC after the addition of 1-pentanol indicates that the alkyl chains in 1-pentanol may contribute to micellization. Compared to water, the number of adsorbed molecules per area (i.e., surface excess) is reduced in the presence of ethanol and 1-pentanol. However, pentanol induces an increased

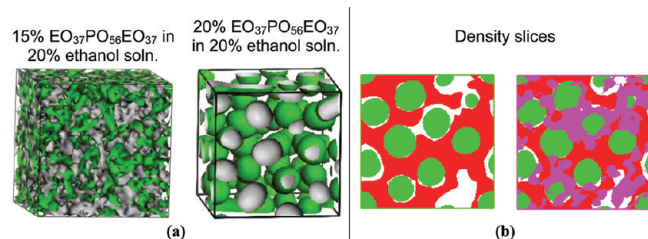


Figure 4. Results after 20 000 steps of a MesoDyn simulation of 15 and 20% by volume of $\text{EO}_{37}\text{PO}_{56}\text{EO}_{37}$ in a 20% ethanol solution at 298 K. The colors indicate PPO (green), PEO (red), and ethanol (magenta), respectively. (a) Iso-surface of the density field for the PPO block, with ethanol, water, and PEO excluded. (b) Cross-sectional slices of the density; ethanol is excluded on the left to highlight the distribution of PEO and PPO blocks.

surface excess when added at the highest concentration used (8 g/L), i.e., the triblock copolymer becomes more surface active.²⁵

The alcohol molecules likely solubilize inside the micelles, producing a relaxation effect on the packing of the polymer chains in the core and the core–corona interface. The alcohol molecules also produce an increase in the hydrophobic character of the PPO blocks and dehydration of the core–corona interface. It has been suggested that below the CMC, the PEO–PPO–PEO copolymer forms unimolecular micelles, where PEO becomes solvated via an expanded coil, while the PPO collapses to a globule that contains a large amount of water.²⁵ When 1-pentanol is present, some molecules could concentrate in the core region (PPO coils) reducing the exposure of PPO groups to water. 1-Pentanol can also replace solvation water around PPO blocks, i.e., it can dehydrate the PPO blocks.²⁵

Phase Morphology of $\text{EO}_{37}\text{PO}_{56}\text{EO}_{37}$ in Aqueous Solution and in the Presence of Alcohols. Figure 3 provides snapshots of the phase morphology after 20 000 steps of a MesoDyn simulation, depending on the volume concentration of $\text{EO}_{37}\text{PO}_{56}\text{EO}_{37}$ in aqueous solution. It is observed that a minimum of 15% volume concentration is required for $\text{EO}_{37}\text{PO}_{56}\text{EO}_{37}$ to form spherical micelles. The association concentration obtained by simulation, however, should be taken on a relative basis since at low concentration, the mean field approximation does not hold well because the phase behavior is controlled by fluctuations. In addition, at low concentrations, the box in the simulation has to be very large in order for micelles to be resolved. Thus, we chose a smaller box and higher concentrations to observe the relative effects of cosolvents on this system. As indicated in Figure 3, while the hydrophobic PPO blocks segregate into the core of the micelles, the hydrophilic PEO blocks disperse in water and form the micellar corona, suggesting that water molecules are extruded from the micellar cores.

Upon increasing the concentration of $\text{EO}_{37}\text{PO}_{56}\text{EO}_{37}$ from 15 to 40%, the number of micelles in the cubic grid decreases from 45 to 20. At the highest polymer concentration, the micelles start to overlap and merge into worm-like shapes. These results agree well with previous MesoDyn simulations¹² that reported a worm-like micelle morphology for $\text{EO}_{37}\text{PO}_{56}\text{EO}_{37}$ in aqueous solution at 50% volume concentration. In addition, these morphologies correspond to the experimental phase diagram.⁵¹ More important is the fact that the threshold in concentration required for observation of associative structures is remarkably high when compared to the experimental values of CMC (see Figure 2 and Table 2).

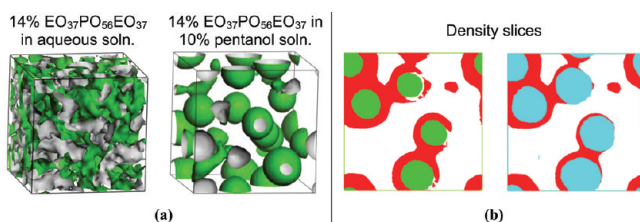


Figure 5. Results after 20 000 steps of a MesoDyn simulation of 14% by volume of EO₃₇PO₅₆EO₃₇ at 298 K. The colors indicate PPO (green), PEO (red), and 1-pentanol (cyan), respectively. (a) Isosurface of the density field of the PPO block for an aqueous system (left) and a 10% pentanol solution (right); 1-pentanol, water, and PEO are excluded. (b) Cross-sectional slices of the density; 1-pentanol is excluded on the left to highlight the distribution of PEO and PPO blocks.

The effects of ethanol and 1-pentanol on the phase behavior of the EO₃₇PO₅₆EO₃₇ solution was also investigated with MesoDyn simulations. To validate the experimental findings, we first focused on the 15% EO₃₇PO₅₆EO₃₇ micellar solution. As indicated in Figure 4a, adding 20% ethanol to the solution prevents the formation of micelles; this behavior is in agreement with the experimental results, which indicated that ethanol increased the CMC. Micelles are formed when the EO₃₇PO₅₆EO₃₇ concentration is increased to 20% at the same alcohol concentration. Two density cross-sectional slices of the 20% EO₃₇PO₅₆EO₃₇ aqueous solution in the presence of 20% ethanol are given in Figure 4b. From these slices, it can be observed that ethanol is solvated by water and is also partially miscible with PEO and even slightly with the PPO blocks. The addition of ethanol improves the solvency for both the PPO and PEO blocks, therefore producing a higher CMC.

The MesoDyn simulation result in the presence of 10% 1-pentanol is given in Figure 5. On the basis of Figure 3 and from the left-most snapshot in Figure 5a, the minimum concentration of EO₃₇PO₅₆EO₃₇ to form micelles in aqueous solution was determined to be 15%. However, micelles are observed in Figure 5a in the presence of 10% 1-pentanol for a EO₃₇PO₅₆EO₃₇ solution at a lower concentration of 14%. Therefore, 1-pentanol decreases the CMC, which also agrees with the experimental results. Cross-sectional density slices for the 14% EO₃₇PO₅₆EO₃₇ aqueous solution with 10% 1-pentanol are given in Figure 5b. These density slices indicate that 1-pentanol prefers to segregate into the hydrophobic PPO micelle core and is also miscible in the surrounding PEO corona. On the basis of the density slices in Figure 5b and compared to the ethanol case in Figure 4b, it can be hypothesized that the alkyl portion of the 1-pentanol molecule contributes to the micelle core formation so that the majority part of 1-pentanol is miscible in the PPO block and thus is one of the reasons that 1-pentanol favors micellization of EO₃₇PO₅₆EO₃₇ in contrast to the effect of ethanol.

Interaction Energy and Radius of Gyration of Micellar Structures. In order to gain further insights into the phase behavior of EO₃₇PO₅₆EO₃₇ in pure water and in the presence of aqueous ethanol and 1-pentanol solutions, MD simulations were performed at 298 K. The interaction energy between the block copolymer and all solvent molecules after equilibrium and the calculated average radius of gyration (R_g) of ten associated EO₃₇PO₅₆EO₃₇ molecules are summarized in Table 3; the interaction energy as a function of time is also given in Figure S1, Supporting Information. Note that a negative value of interaction energy indicates attraction between the two entities. Table 3 and

Table 3. Average Values in Various Aqueous/Alcohol Solutions of the Radius of Gyration (R_g) of EO₃₇PO₅₆EO₃₇ Micelles and the Interaction Energy between the Solvent and the Block Copolymers^a

	water	water + ethanol	water + 1-pentanol
interaction energy (kcal/mol)	-5100 ± 275	-5420 ± 290	-4250 ± 200
R_g (Å)	21.1 ± 4.6	23.8 ± 4.2	23.2 ± 3.4

^a The values were averaged over the last 10 ns of the simulations.

Figure S1, Supporting Information, indicate that the interaction energy between EO₃₇PO₅₆EO₃₇ and water with ethanol is stronger, whereas the addition of 1-pentanol produces the opposite effect. For R_g a slight increase was observed with the inclusion of both ethanol and 1-pentanol.

In general, ethanol was a good solvent for both the PEO and PPO blocks, which resulted in the water and ethanol mixture being a better solvent than pure water for EO₃₇PO₅₆EO₃₇, as indicated by the increase in the interaction energy between EO₃₇PO₅₆EO₃₇ and the solvent molecules with the addition of ethanol. In a good solvent, the polymer chains tend to be more extended and maximize the number of polymer–solvent contacts, leading to large R_g values. In a poor solvent, the polymer segments contract or even collapse, in order to minimize interactions with the solvent. From the R_g values in Table 3, ethanol–water solutions lead to a slightly larger R_g than pure water, which indicates better solvency for EO₃₇PO₅₆EO₃₇. This observation also suggests why it was observed in the experiments and the MesoDyn simulations that the addition of ethanol increases the critical micelle concentration.

When adding 1-pentanol into water, however, a decrease of interaction energy between EO₃₇PO₅₆EO₃₇ was observed, suggesting that solvency in water decreased for EO₃₇PO₅₆EO₃₇. Overall, these results are in agreement with the experimental observations above and also with the MesoDyn simulations: 1-pentanol induces the formation of micelles in EO₃₇PO₅₆EO₃₇ aqueous solution, while ethanol produces the reverse effect. However, from the R_g values in Table 3, 1-pentanol–water solutions lead to a slightly larger R_g than pure water. Since this increase cannot be attributed to better solvency, another molecular mechanism is likely in play. Since the 1-pentanol is highly hydrophobic due to its alkyl chain, it is likely to prefer to be associated with the copolymer instead of the water. Within the copolymer, it is much more likely to associate with the hydrophobic block, PPO, than the hydrophilic one. Therefore, the presence of the 1-pentanol in the PPO core likely increased its overall R_g value by loosening the packing of the polymer chains. A similar mechanism was also proposed by Caragheorgheopol and co-workers⁵² based on experimental observations on a series of alcohols with aqueous EO₂₇PO₃₉EO₂₇. They also noted that the hydration of the PEO shell of the micelle was reduced with the incorporation of the alcohols with moderate alkyl components due to the increased hydrophobic character of the core.

Interestingly, a recent study by Parekh and Bahadur⁵³ indicated through dynamic light scattering measurements of a series of PEO–PPO–PEO block copolymers with alkanols (as well as alkoxyethanols and alkanediols) that the hydrodynamic diameter of the micelles changed as a function of the alcohol type. They found that short chain alkanols tend to remain in the aqueous phase but increased the hydrodynamic radius due to the solvation

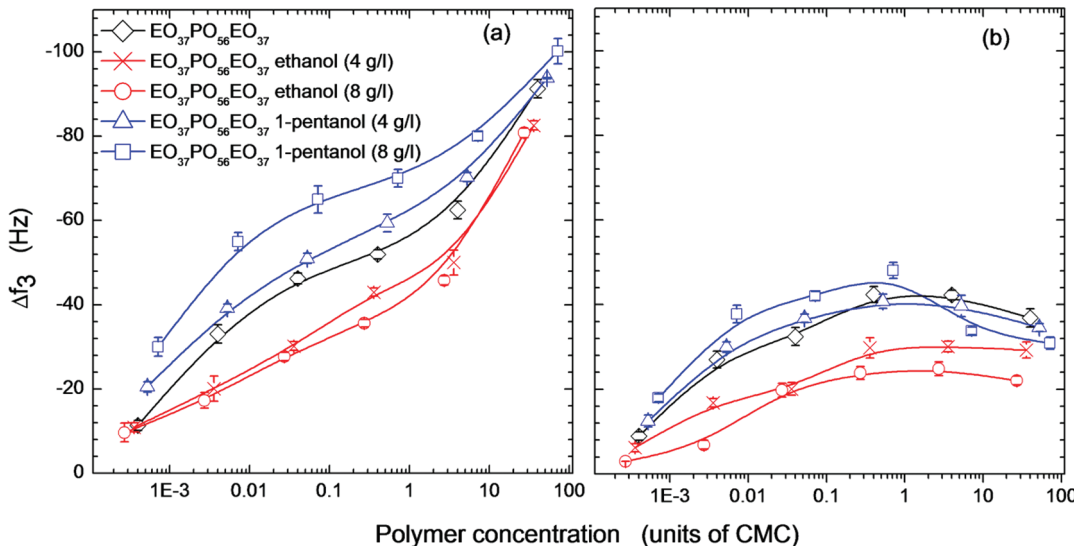


Figure 6. QCM 3rd overtone frequency profiles (Δf_3) for PP upon $\text{EO}_{37}\text{PO}_{56}\text{EO}_{37}$ adsorption from water (\diamond), ethanol (4 (\times) and 8 g/L (\circ)), and 1-pentanol (4 (\triangle) and 8 g/L (\square)) solutions before (a) and after (b) rinsing with water. The experimental standard deviation for all data collected is shown as error bars at each condition. The solid lines are meant to guide the eye.

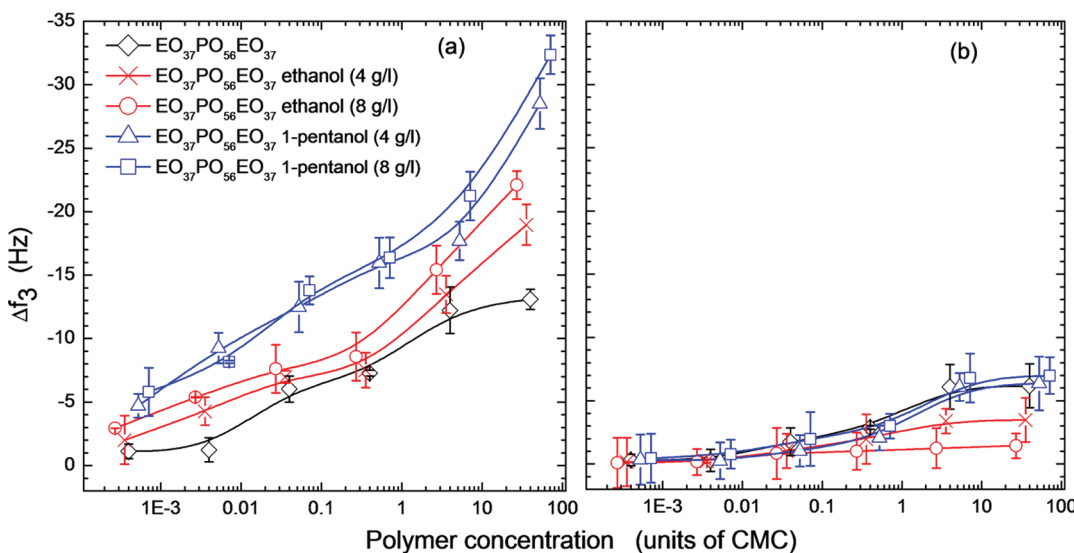


Figure 7. QCM 3rd overtone frequency profiles (Δf_3) for cellulose upon $\text{EO}_{37}\text{PO}_{56}\text{EO}_{37}$ adsorption from water (\diamond), ethanol (4 (\times) and 8 g/L (\circ)), and 1-pentanol (4 (\triangle) and 8 g/L (\square)) solutions. Data before (a) and after (b) rinsing with water are included. The experimental standard deviation for all data collected is shown as error bars at each condition. The solid lines are meant to guide the eye.

of the PEO shell (similarly to what is depicted in Figure 4b). For medium and longer chain alkanols, the alcohols penetrated into the micelle (similarly to what is depicted in Figure 5b), resulting in micelle growth as the concentration of the alcohol increases. These preferential interactions of the alcohols and their impact on the PEO–PPO–PEO block copolymers are also supported from an extensive thermodynamic analysis performed by Cheng and Jolicœur.⁵⁴

Adsorption of $\text{EO}_{37}\text{PO}_{56}\text{EO}_{37}$ in the Presence of Alcohols. Figure 6 includes isotherms of $\text{EO}_{37}\text{PO}_{56}\text{EO}_{37}$ adsorbing onto hydrophobic PP in the presence of alcohols before (Figure 6a) and after (Figure 6b) rinsing with water. The frequency shifts after rinsing indicate the removal of loosely bound $\text{EO}_{37}\text{PO}_{56}\text{EO}_{37}$ molecules; a large number of segments remains adsorbed

on the surfaces. The adsorption isotherms for $\text{EO}_{37}\text{PO}_{56}\text{EO}_{37}$ on hydrophobic PP in the presence of shorter chain alcohols (ethanol) are similar to those of $\text{EO}_{37}\text{PO}_{56}\text{EO}_{37}$ adsorbed from pure water, except that the adsorption amount of $\text{EO}_{37}\text{PO}_{56}\text{EO}_{37}$ is reduced in the presence of ethanol, depending on the alcohol concentration. Shorter chain alcohols (ethanol) increase the solvation of PEO groups and improved solvency. The presence of longer chain alcohols (i.e., 1-pentanol) increases the adsorbed amount of $\text{EO}_{37}\text{PO}_{56}\text{EO}_{37}$ when applied at submicellar concentrations, while it reduces polymer adsorption at concentrations above the CMC. This observation can also be explained by the surface tension and Gibbs free energy values discussed before from Table 2; the longer chain alcohols (i.e., 1-pentanol) reduce solvency and facilitate polymer association or formation of $\text{EO}_{37}\text{PO}_{56}\text{EO}_{37}$

micelles. For concentrations of $\text{EO}_{37}\text{PO}_{56}\text{EO}_{37}$ copolymer above the CMC, the release of $\text{EO}_{37}\text{PO}_{56}\text{EO}_{37}$ molecules adsorbed onto PP surfaces is more limited if micelles form in the presence of 1-pentanol. There are also higher energy requirements for adsorption of the molecules because they need to dissociate into unimers (which is already difficult due to the hydrophobic effect); then, they have to diffuse to the interface and adsorb onto PP surfaces (which also requires energy). If the energy required for adsorption is higher than that for disrupting a micelle, then the molecules remain associated. Below the CMC, only unimers are present, and they can adsorb with the PPO and PEO groups hydrated. In contrast, the hydration above the CMC is restrained due to the fact that water around the polymer molecules is replaced by 1-pentanol.

The adsorption isotherms for $\text{EO}_{37}\text{PO}_{56}\text{EO}_{37}$ on hydrophilic cellulose are given in Figure 7. The figure includes data in the presence of alcohols before (Figure 7a) and after (Figure 7b) rinsing with water. A similar effect of rinsing is observed in all cases. Except for the case of adsorption from ethanol-containing solution, all adsorption isotherms show a sharp increase in the extent of adsorption at around the CMC. In the presence of ethanol, the adsorbed amount is more limited compared with that from pure water. This observation can be explained by better solvency effect of ethanol, relative to other alcohols, as pointed out earlier. Ethanol favors expansion of the PEO groups in the polymer molecules (better solvency); more expanded molecules have less bound water (dehydration of PEO groups) than coiled ones, which lead to a flatter conformation of the molecules on the surface and therefore lower adsorbed amount.

In order to compare the respective adsorbed masses, the shifts in frequency (QCM) after rinsing were converted into adsorbed

mass by using eq 1. Table 4 summarizes the results of such calculation for all surfaces exposed to aqueous solutions of $\text{EO}_{37}\text{PO}_{56}\text{EO}_{37}$ in pure water and in the presence of alcohols at maximum adsorption concentration, after rinsing with water. The extent of surface coverage at saturation at the PP–liquid and cellulose–liquid interfaces obtained by QCM is much lower, as expected, when compared with results obtained at the air–liquid interface where a tighter packing is observed. This observation is likely due to the higher configurational entropic penalty sustained by the copolymers at solid surfaces compared to the more diffuse air–water interface. In addition, at saturation the adsorbed copolymer amount increases on both the PP and cellulose surfaces in the presence of 1-pentanol, while it decreases in the presence of ethanol. Adding ethanol improves solvency and limits the adsorption of $\text{EO}_{37}\text{PO}_{56}\text{PO}_{37}$, while 1-pentanol promotes the adsorption on PP and cellulose.

Adsorption of $\text{EO}_{37}\text{PO}_{56}\text{PO}_{37}$ on PP Surfaces from Multiscale Simulations. Adsorption of $\text{EO}_{37}\text{PO}_{56}\text{EO}_{37}$ on a PP surface was investigated with MesoDyn simulations. The morphologies of systems consisting of 20% of $\text{EO}_{37}\text{PO}_{56}\text{EO}_{37}$ in different solvents and sandwiched between two PP layers are given in Figure 8. For 20% $\text{EO}_{37}\text{PO}_{56}\text{EO}_{37}$ in pure water (Figure 8a), the entire copolymer segregates to and adsorbs onto the PP surfaces; the PPO blocks closely contact the PP surfaces and form layers at the top and bottom directions because of the box periodicity. The PEO blocks stay outside PPO and form the second layer near the PP surface, with all the water located in the middle of the box. These simulation results suggest that $\text{EO}_{37}\text{PO}_{56}\text{EO}_{37}$ tends to adsorb onto the PP surface in pure water. In the system containing 20% ethanol (Figure 8b), spherical micelles exist and indicate less $\text{EO}_{37}\text{PO}_{56}\text{EO}_{37}$ adsorbed on the PP surfaces; there are still some polymers left as micelles in bulk solution. Therefore, adding ethanol decreases the amount of $\text{EO}_{37}\text{PO}_{56}\text{EO}_{37}$ absorbing onto the PP surface, in agreement with the experimental results. For the aqueous solution with 10% 1-pentanol (Figure 8c), $\text{EO}_{37}\text{PO}_{56}\text{EO}_{37}$ is observed to absorb onto the PP surface, and 1-pentanol appears to associate with the PPO and PEO blocks, as observed without the PP surfaces in Figure 5. However, a strong contrast to Figure 5 is that no micelles are observed to form in solution; thus, the adsorbed 1-pentanol may contribute to the increased adsorbed amount onto the PP surface. However, the experimental data from QCM shows the adsorption amount of $\text{EO}_{37}\text{PO}_{56}\text{EO}_{37}$ reduced at concentrations above CMC, which may be due to the large amount of water that was excluded from the adsorbed layer.

Table 4. $\text{EO}_{37}\text{PO}_{56}\text{PO}_{37}$ Adsorbed Mass on Cellulose (0.1% w/v $\text{EO}_{37}\text{PO}_{56}\text{PO}_{37}$) and on PP (10% w/v $\text{EO}_{37}\text{PO}_{56}\text{PO}_{37}$) from Water and in the Presence of Alcohols after Rinsing

	maximum packing (ng/cm ²)	PP (ng/cm ²)	cellulose (ng/cm ²)
water	420	250	36.4
4 g/L ethanol + water	399	175.8	20.5
8 g/L ethanol + water	269	140.8	8.4
4 g/L 1-pentanol + water	193	240.7	37.6
8 g/L 1-pentanol + water	366	283.8	41.2

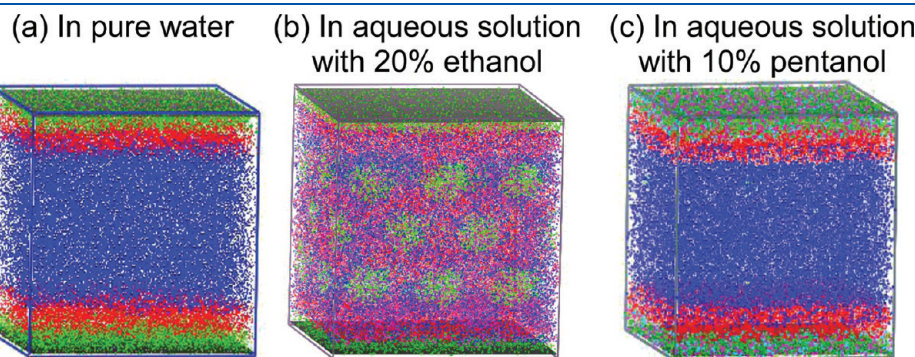


Figure 8. Simulation snapshots of 20% $\text{EO}_{37}\text{PO}_{56}\text{EO}_{37}$ polymer in solution at 298 K after 1 ms of a MesoDyn simulation. The colors indicate the density fields of PPO (green), PEO (red), and water (blue); magenta is ethanol in panel b and is 1-pentanol in panel c. The PP layer (not shown) is positioned at the top of the simulation box; with periodic boundary conditions, the system will see this layer at the bottom of the box also, hence the symmetry in the snapshots.

Table 5. Interaction Energy between PP and EO₃₇PO₅₆EO₃₇ or Alcohol Molecules in Water or Water-Alcohol Solutions^a

molecule	water		water + ethanol		water + 1-pentanol	
	EO ₃₇ PO ₅₆ EO ₃₇	EO ₃₇ PO ₅₆ EO ₃₇	ethanol	EO ₃₇ PO ₅₆ EO ₃₇	1-pentanol	
interaction energy (kcal/mol)	−355 ± 25	−288 ± 21	−110 ± 26	−350 ± 20	−250 ± 21	

^a The values were averaged over the last 10 ns of the simulations.

To better understand EO₃₇PO₅₆EO₃₇ adsorption on PP, MD simulations were also performed. After equilibrium, the average interaction energies were calculated between the PP surface and either EO₃₇PO₅₆EO₃₇ or the alcohol molecules; these values are given in Table 5. Adding 1-pentanol does not change the interaction energy between the block copolymer and the PP. However, the presence of ethanol decreases the attractive interaction energy by 20%, which results in reduced adsorption of EO₃₇PO₅₆EO₃₇ onto the PP surface. In addition, the interaction energy between ethanol and the PP surface is over half less attractive than the interaction of 1-pentanol and the PP surface. These results explain the results in Figure 8 that the addition of ethanol reduces the amount of EO₃₇PO₅₆EO₃₇ segregating near the PP surface, but introducing 1-pentanol produces few changes.

CONCLUSIONS

The association of EO₃₇PO₅₆EO₃₇ in aqueous solution and the adsorption on PP and cellulose in the presence and absence of alcohols were investigated and compared by using experimental and computer simulation methods. The presence of a shorter chain alcohol (ethanol) prevented the formation of micelles in bulk solution and also reduced the adsorbed amount of EO₃₇PO₅₆EO₃₇ on both hydrophobic and hydrophilic surfaces. The presence of a longer chain alcohol (1-pentanol) favored the micellization in aqueous solution and increased the adsorbed amount of EO₃₇PO₅₆EO₃₇ on the hydrophobic surface at submicellar EO₃₇PO₅₆EO₃₇ concentrations, while the adsorbed amount was reduced when EO₃₇PO₅₆EO₃₇ concentration is above CMC. The presence of 1-pentanol had little effect on the adsorbed amount of EO₃₇PO₅₆EO₃₇ on the hydrophilic cellulose surface.

ASSOCIATED CONTENT

Supporting Information. Interaction energy between the block copolymer and solvent molecules calculated from the MD trajectory. This material is available free of charge via the Internet at <http://pubs.acs.org>.

AUTHOR INFORMATION

Corresponding Author

*E-mail: ojrojas@ncsu.edu (O.J.R.); melissa_pasquinelli@ncsu.edu (M.A.P.).

ACKNOWLEDGMENT

This work was partially supported by NC State University Nonwovens Cooperative Research Center under Project numbers 07-98 and 08-112. Dr. Alex Goldberg (Accelrys) is gratefully acknowledged for helpful discussions.

REFERENCES

- (1) BASF Technical Brochure; BASF Co.: Parsippany, NJ, 1989.
- (2) Muller, R. H. *Modification of Drug Carriers. Colloidal Carriers for Controlled Drug Delivery and Targeting*; CRC Press: Boca Raton, FL, 1991; p 23.
- (3) Foster, B.; Cosgrove, T.; Espidel, Y. *Langmuir* **2009**, *25*, 6767–6771.
- (4) Chakraborty, A. K.; Golumbfksie, A. *Annu. Rev. Phys. Chem.* **2001**, *52*, 537–573.
- (5) Muthukumar, M.; Ober, C. K.; Thomas, E. L. *Science* **1997**, *277*, 1225–1232.
- (6) Peppas, N. A.; Langer, R. *Science* **1994**, *263*, 1715–1719.
- (7) Brandai, P.; Stroeve, P. *Macromolecules* **2003**, *36*, 9492–9501.
- (8) Liu, X.; Wu, D.; Turgman-Cohen, S.; Genzer, J.; Theyson, T. W.; Rojas, O. J. *Langmuir* **2010**, *26*, 9565–9574.
- (9) Green, R. J.; Tasker, S.; Davies, J.; Davies, M. C.; Rojberts, C. J.; Tendler, S. J. B. *Langmuir* **1997**, *13*, 6510–6515.
- (10) Fraaije, J. G. E. M.; Zvelindovsky, A. V.; Sevink, G. J. A.; Maurits, N. M. *Mol. Simul.* **2000**, *25*, 131–144.
- (11) Lam, Y.-M.; Goldbeck-Wood, G. *Polymer* **2003**, *44*, 3593–3605.
- (12) Fraaije, J. G. E. M.; Zvelindovsky, A. V.; Sevink, G. J. A. *Mol. Simul.* **2004**, *30*, 225–238.
- (13) Li, Y. Y.; Hou, T. J.; Guo, S. L.; Wang, K. X.; Xu, X. *J. Chem. Phys.* **2000**, *15*, 2749–2753.
- (14) Guo, S. L.; Hou, T. J.; Xu, X. *J. Phys. Chem. B* **2002**, *106*, 11397–11403.
- (15) Yang, S.; Yuan, S.; Zhang, X.; Yan, Y. *Colloids Surf., A* **2008**, *322*, 87–96.
- (16) Zhao, Y. R.; Chen, X.; Yang, C. J.; Zhang, G. D. *J. Phys. Chem. B* **2007**, *111*, 13937–13942.
- (17) Liu, H.; Li, Y.; Krause, W. E.; Pasquinelli, M. A.; Rojas, O. J. Submitted for publication.
- (18) Kipkemboi, P.; Fogden, A.; Alfredsson, V.; Flodström, K. *Langmuir* **2001**, *17*, 5398–5402.
- (19) Alexandridis, P.; Yang, L. *Macromolecules* **2000**, *33*, 5574–5587.
- (20) Armstrong, J.; Chowdhry, B.; Mitchell, J.; Beezer, A.; Leharne, S. *J. Phys. Chem.* **1996**, *100*, 1738–1745.
- (21) Ivanova, R.; Alexandridis, P.; Lindman, B. *Colloids Surf., A* **2001**, *41*, 183–185.
- (22) Ivanova, R.; Lindman, B.; Alexandridis, P. *Langmuir* **2000**, *16*, 3660–3675.
- (23) Alexandridis, P.; Holzwarth, J.; Hatton, T. A. *Macromolecules* **1994**, *27*, 2414–2425.
- (24) Sharp, M. A.; Washington, C.; Cosgrove, T. *J. Colloid Interface Sci.* **2010**, *344*, 438–446.
- (25) Su, Y.; Wei, X.; Liu, H. *Langmuir* **2003**, *19*, 2995–3000.
- (26) Alexandridis, P.; Yang, L. *Macromolecules* **2000**, *33*, 5574–5587.
- (27) Armstrong, J.; Chowdhry, B.; Mitchell, J.; Beezer, A.; Leharne, S. *J. Phys. Chem.* **1996**, *100*, 1738–1745.
- (28) Song, J.; Liang, J.; Liu, X.; Krause, W. E.; Hinestroza, J. P.; Rojas, O. J. *Thin Solid Films* **2009**, *517*, 4348–4354.
- (29) Sauerbrey, G. Z. *Angew. Phys.* **1959**, *155*, 206–222.
- (30) Edvardsson, M.; Rodahl, M.; Kasemo, B.; Höök, F. *Anal. Chem.* **2005**, *77*, 4918–4926.
- (31) Rodahl, M.; Kasemo, B. *Sens. Actuators, B* **1996**, *37*, 111–116.
- (32) Plimpton, S. *J. Comput. Phys.* **1995**, *117*, 1.
- (33) Material Studio; Accelrys Software: San Diego, CA, 2004.
- (34) Sun, H.; Ren, P.; Fried, J. R. *Comput. Theor. Polym. Sci.* **1998**, *8*, 229–246.

- (35) van Vlimmeren, B. A. C.; Maurits, N. M.; Zvelindovsky, A. V.; Sevink, G. J. A.; Fraaije, J. G. E. M. *Macromolecules* **1999**, *32*, 646–656.
- (36) Fraaije, J. G. E. M.; van Vlimmeren, B. A. C.; Maurits, N. M.; Postma, M.; Evers, O. A.; Hoffmann, C.; Altevogt, P.; Goldbeck, W. G. *J. Chem. Phys.* **1997**, *106*, 4260–4269.
- (37) Fraaije, J. G. E. M. *J. Chem. Phys.* **1993**, *99*, 9202–9212.
- (38) Malmsten, M.; Linse, P.; Cosgrove, T. *Macromolecules* **1992**, *25*, 2474–2481.
- (39) Malmsten, M.; Linse, P.; Zhang, K. W. *Macromolecules* **1993**, *26*, 2905–2910.
- (40) Svensson, M.; Alexandridis, P.; Linse, P. *Macromolecules* **1999**, *32*, 637–645.
- (41) Hill, T. L. *An Introduction to Statistical Thermodynamics*; Dover Publications: New York, 1960.
- (42) Zhang, M.; Choi, P.; Sundararaj, U. *Polymer* **2003**, *44*, 1979–1986.
- (43) Mayo, S. L.; Olafson, B. D.; Goddard, W. A. *J. Phys. Chem.* **1990**, *94*, 8897–8909.
- (44) Fan, Z. J.; Williams, M. C.; Choi, P. *Polymer* **2002**, *43*, 1497–1502.
- (45) Maurits, N. M.; van Vlimmeren, B. A. C.; Fraaije, J. G. E. M. *J. Phys. Rev. E* **1997**, *56*, 816–825.
- (46) van Vlimmeren, B. A. C.; Fraaije, J. G. E. M. *Comput. Phys. Commun.* **1996**, *99*, 21–28.
- (47) Reimhult, E.; Larsson, C.; Kasemo, B.; Höök, F. *Anal. Chem.* **2004**, *76*, 7211–7220.
- (48) Lin, Y. N.; Alexandridis, P. *Langmuir* **2002**, *18*, 4220–4231.
- (49) Hammouda, B. *Adv. Polym. Sci.* **1993**, *106*, 87–133.
- (50) Hammouda, B. *J. Polym. Sci., Part B: Polym. Phys.* **2006**, *44*, 3195–3199.
- (51) Alexandridis, P.; Zhou, D.; Khan, A. *Langmuir* **1996**, *12*, 2690–2700.
- (52) Caragheorgheopol, A.; Caldara, H.; Dragutan, H.; Joela, H.; Brown, W. *Langmuir* **1997**, *13*, 6912–6921.
- (53) Parekh, P.; Bahadur, P. *J. Surfactants Deterg.* **2011**, *14*, 425–431.
- (54) Cheng, Y.; Jolicœur, C. *Macromolecules* **1995**, *28*, 2665–2672.